Focused Crossed Andreev Reflection

Håvard Haugen and Arne Brataas
Department of Physics, Norwegian University of Science and Technology, N-7491 Trondheim, Norway

Xavier Waintal
SPSMS-INAC-CEA, 17 rue des Martyrs, 38054 Grenoble CEDEX 9, France

Gerrit E. W. Bauer
Kavli Institute of NanoScience, Delft University of Technology, 2628 CJ Delft, The Netherlands
(Dated: July 28, 2010)

We consider non-local transport in a system with one superconducting and two normal metal terminals. Electron focusing by weak perpendicular magnetic fields is shown to tune the ratio between crossed Andreev reflection (CAR) and electron transfer (ET) in the non-local current response. Additionally, electron focusing facilitates non-local signals between normal metal contacts where the separation is as large as the mean free path rather than being limited by the coherence length of the superconductor. CAR and ET can be selectively enhanced by modulating the magnetic field.

PACS numbers: 74.45.+c, 73.63.-b, 74.25.Fy

Andreev reflection (AR) is a signature sub-gap scattering phenomena at normal-superconductor (NS) interfaces. Two electrons (at energies symmetrically around the chemical potential of the superconductor) enter the superconducting condensate as a Cooper pair, resulting in a retro-reflected hole on the normal side of the interface. The superconducting coherence length ξ determines the spatial extent of the Cooper pairs and therefore gives the scale of the largest possible separation between the incoming electron and the retro-reflected hole (at the interface).

When two normal metal contacts N_1 and N_2 separated by a distance $L \leq \xi$ are connected to a superconductor, the Andreev reflected holes arising from incoming electrons in N_1 also have a finite probability of leaving the structure through N_2 [1–4]. This non-local process, called crossed Andreev reflection (CAR), creates a spatially separated phase-coherent electron-hole pair, and is a candidate for a solid state entangler [5]. Competing with CAR is a process called electron transfer (ET), in which an electron propagates from N_1 to N_2 either directly or via a virtual excitation in the superconductor [2]. The second process, involving a virtual excitation, is also referred to as electron co-tunneling. The competition between CAR and ET has been studied for about a decade [1–3, 5–11]. Theoretical papers report that ET typically dominates CAR in linear response [3, 9]. CAR can dominate ET beyond linear response or in the presence of interactions [8, 10, 12, 13].

Much work on CAR has focused on the spin manipulation of the carriers, with normal contact separation L limited by the superconducting coherence length ξ [2, 3, 5, 7, 11, 14]. In this Letter, we study electron and hole focusing by a weak perpendicular magnetic field in a high-mobility two-dimensional electron gas (2DEG) [15]

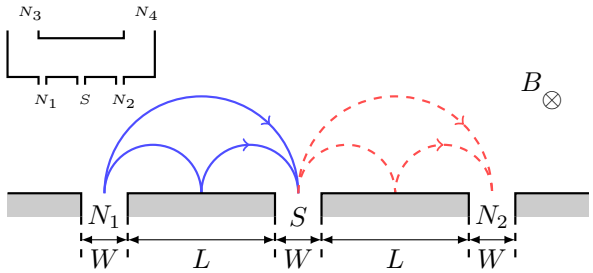

(a) Focused crossed Andreev reflection

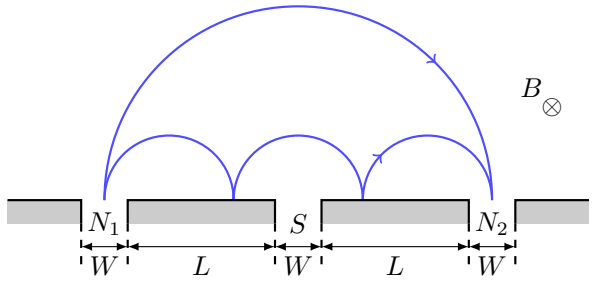

(b) Focused electron transfer

FIG. 1. (Color online) Illustration of focused crossed Andreev reflection. (a) When the separation between N_1 and N_2 is an even integer multiple of the cyclotron diameter d_c, electron focusing enhances CAR and leads to a negative non-local conductance. (b) When the separation is an odd multiple of d_c, ET is enhanced and we expect a positive peak in the non-local conductance. Inset of (a): Device used in the simulations.

We attach a single superconducting contact between two normal contacts along the edge of the device. In our scheme AR induces electron-hole correlations on length scales which are only limited by the mean free path $l_{\rm mf}$ rather than ξ. For typical superconductors, ξ lies between 10 nm and 100 nm, [12] while $l_{\rm mf}$ can reach several

microns in 2DEGs [16] Very high mobilities have also been reported for graphene [17, 18], which is another candidate for focused CAR. The tuning between CAR and ET through the external magnetic field is possible through the orbital degrees of freedom at field strengths that do not introduce a spin selectivity of the contacts. As long as the field is smaller than the critical field of the superconductor, the relative magnitude of CAR and ET can be controlled by varying the magnetic field.

The basic mechanism is illustrated in Fig. 1. An electron is injected from the left contact N_1 by a small voltage bias. For weak magnetic fields, the motion of the electrons and holes can be understood in terms of semiclassical cyclotron orbits [15, 19] as a result of the Lorentz force. For certain magnetic field strengths (Fig. 1a), the electrons from N_1 are focused on the superconducting center contact S, at which an Andreev reflected hole is emitted. Since AR changes the sign of both charge and effective mass, the holes will feel the same Lorentz force as the electrons and are therefore focused on contact N_2 to the right of S at the same distance as N_1 [19–21]. The probability for CAR is thus enhanced at the cost of ET. On the other hand, ET is enhanced at certain other magnetic fields at which the incoming electrons are focused on N_1, but where the skipping orbits do not interact with the superconductor (Fig. 1b).

Andreev reflection in the presence of a magnetic field has been thoroughly studied in the literature [19–24]. Electron focusing has been used for the first direct observation of Andreev reflection at an NS interface [19, 22]. Resonant enhancement of CAR due to Andreev bound states at an NS interface has been proposed [23, 24]. Recently, an Andreev interferometer was used to demonstrate the phase coherent nature of CAR and ET [11]. We show here that electron focusing clearly discriminates between CAR and ET, which might be useful to maximize entanglement generation in artificial solid state devices.

Before delving into the fully quantum mechanical treatment, we now discuss the physics of electron focusing in a semi-classical picture. The length scale associated with the semi-classical motion of electrons with momentum $\hbar k_F$ in a magnetic field B is the cyclotron radius r_c for electrons at the Fermi surface. As seen from Fig. 1, the natural parameter in electron focusing is the cyclotron diameter

$$d_c = \frac{2\hbar k_F}{eB}, \tag{1}$$

where we assume high mobility, i.e. $d_c \ll l_{\rm mf}$ [15]. Electron focusing between the normal contacts in Fig. 1 occurs when the distance $2L$ between N_1 and N_2 is an integer multiple of the cyclotron diameter, $2L = nd_c$, where n is a positive integer. ET is enhanced for odd n, while CAR will be enhanced for even n. The focusing field [15],

$$B_{\rm focus} = \frac{2\hbar k_F}{eL}, \tag{2}$$

determines the magnetic field scale for which focusing features can be expected.

For strong magnetic fields the system enters the quantum Hall (QH) regime, where the charge carriers are better described as chiral edge states than semi-classical skipping orbits [16]. The characteristic length scale associated with the QH regime is the magnetic length l_B, which is the radius of the disc that encloses one flux quantum, $\pi l_B^2 B = \Phi_0 = h/2e$. To avoid the QH regime, the magnetic flux density $n_B = 1/(\pi l_B^2)$ must be substantially lower than the electron density $n = k_F^2/(2\pi)$, or $B \ll \frac{h}{2e} n \approx 7$ T, for typical values for the electron density in a 2DEG, $n \approx 3.5 \times 10^{15}$ m^{-2} (corresponding to $\lambda_F \approx 40$ nm) [15]. Superconductors with upper critical fields above 10 T are readily available [25]. We expect CAR to be enhanced also in the QH regime, since the edge states will be forced to interact with the superconductor on the way from N_1 to N_2.

We will now confirm the semi-classical predictions by a numerical quantum calculation of the non-local transport properties of the device shown in Fig. 1. The competition between CAR and ET is studied through the non-local conductance [3, 9],

$$G_{21} \stackrel{\rm def.}{=} -\frac{\partial I_2}{\partial V_1} = G_{21}^{\rm ET} - G_{21}^{\rm CAR}, \tag{3}$$

where I_2 is the current response in contact N_2 due to the application of a voltage V_1 in the normal metal contact N_1 while N2 and S are grounded. The overall minus sign is due to the definition of the currents to be positive when electrons leave the reservoirs. The difference in sign of $G_{21}^{\rm ET}$ and $G_{21}^{\rm CAR}$ in Eq. (3) is due to the fact that the outgoing current in N_2 produced by ET consists of negatively charged electrons, while CAR contributes with positively charged holes.

In our calculation we employ the standard 2DEG Hamiltonian

$$\mathcal{H}(\boldsymbol{r}) = \frac{\boldsymbol{p}^2}{2m} + V(\boldsymbol{r}) - \mu, \tag{4}$$

where $\boldsymbol{p} = -i\hbar\nabla + e\boldsymbol{A}(\boldsymbol{r})$ is the canonical momentum and m the effective mass. The Hamiltonian (4) is extended it to Nambu space [26]

$$H = \int {\rm d}\boldsymbol{r}\ \Psi^\dagger(\boldsymbol{r}) \begin{pmatrix} \mathcal{H}(\boldsymbol{r}) & \Delta(\boldsymbol{r}) \\ \Delta^*(\boldsymbol{r}) & -\mathcal{H}^*(\boldsymbol{r}) \end{pmatrix} \Psi(\boldsymbol{r}), \tag{5}$$

where at the contact S the superconducting pair potential $\Delta(\boldsymbol{r})$ is assumed to vary abruptly on the scale of the Fermi wavelength λ_F, and is therefore modelled as step function which is non-zero only inside the center contact S. All energies are measured from the chemical potential μ of the superconductor. The Nambu spinor Ψ is defined in terms of the field operators ψ as $\Psi = (\psi, \psi^\dagger)^T$. A perpendicular magnetic field $\boldsymbol{B} = \nabla \times \boldsymbol{A} = B\boldsymbol{e}_z$ is included everywhere except in the superconductor, which expels the field [27], and we consider only elastic scattering.

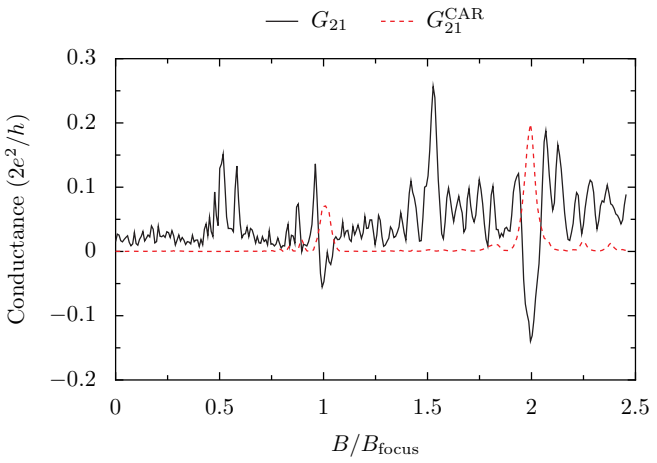

FIG. 2. (Color online) Non-local conductance G_{21} (solid black) for a device with point contacts ($W \approx \lambda_F/2$). The magnetic field is given in units of the focusing field $B_{\mathrm{focus}} = 0.406$ T. The contribution from G_{21}^{CAR} (dashed red) shows that the negative peaks in G_{21} are evidence for CAR at integer multiples of B/B_{focus}.

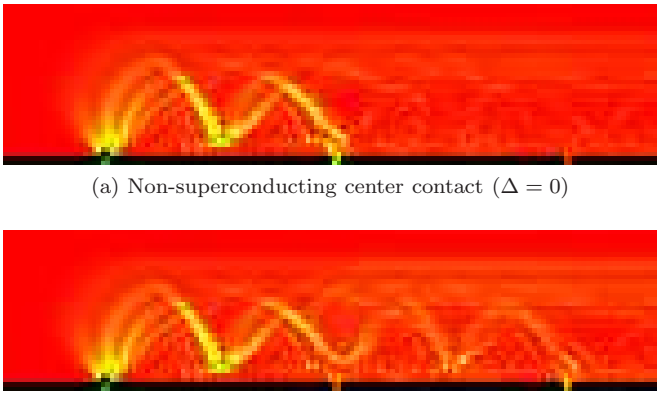

(a) Non-superconducting center contact ($\Delta = 0$)

(b) Superconducting center contact ($\Delta \neq 0$)

FIG. 3. (Color online) Electronic current density in a perpendicular magnetic field at $T = 1$ K. Two skipping orbits, corresponding to a magnetic field $B \approx 2fB_{\mathrm{focus}}$, are clearly visible. (a) With a non-superconducting center contact S, a large portion of the current injected through contact N_1 leaves the structure through S. (b) When S is superconducting, the Andreev reflected holes from S contribute to the current from S to N_2.

At zero temperature, quantum interference due to scattering at the sharp boundaries close to the contacts can mask the electron focusing effect [15]. We therefore calculate the non-local differential conductance at finite temperature, using the standard formula,

$$G_{ij} = \int \mathrm{d}\varepsilon \; G_{ij}(\varepsilon) \left(-\frac{\partial n_F(\varepsilon)}{\partial \varepsilon} \right), \qquad (6)$$

where n_F is the Fermi-Dirac distribution function.

We use the knitting algorithm presented in Ref. 28 to calculate the self energies and retarded and advanced Green functions. Standard expressions relate the conductance and current density to these quantities. The device used in the simulations is sketched in the inset of Fig. 1a, where the two auxiliary contacts N_3 and N_4 are added to prevent back-reflection of electrons into N_1. All edges cause specular electron scattering only.

Figure 2 shows the calculated non-local conductance from Eq. (6) as a function of perpendicular magnetic field at a temperature of $T = 1$ K. The value chosen for the pair potential Δ would correspond to Pb, which has a critical temperature of $T_c \approx 7\,\mathrm{K} \gg T$ [29]. Also, since $T < T_c/2$, we disregard the temperature dependence of the pair potential, $\Delta(T) \approx \Delta(0)$ [30].

The injector N_1, superconducting S, and collector N_2 contacts are point contacts with width $W \approx \lambda_F/2$, so that only a single mode contributes to the current [16]. The distance $L = 500$ nm between the contacts corresponds to a focusing field of $B_{\mathrm{focus}} = (0.39 \pm 0.02)$ T, where the uncertainty is due to the finite width W of the contacts relative to L. The value found in the simulation agrees with the expectation within the uncertainty dictated by the finite size of the contacts.

The enhancement of CAR due to electron focusing is clearly seen in terms of the two negative peaks in Fig. 2. The position of these peaks at integer values of B/B_{focus} and the explicit calculation of the contribution from G_{21}^{CAR} in Eq. (3) (dashed red line) is consistent with the semi-classical interpretation presented earlier. The expected enhancement of ET at half-integer B/B_{focus} is somewhat masked by interference peaks, but the positive peaks in G_{21} when B/B_{focus} equals 1/2 and 3/2 are clearly visible. As the magnetic field increases beyond $2.5\,B_{\mathrm{focus}}$, the system gradually enters the QH regime, where transport is associated with chiral edge states.

The focusing enhancement of CAR at $B/B_{\mathrm{focus}} = 1$ and 2 in Fig. 2 can be visualized by calculating the charge current density due to electrons injected from contact N_1. This is shown in Fig. 3, where we have set $B \approx 2B_{\mathrm{focus}}$. A skipping orbit between N_1 and S is clearly visible. Also visible is the diffraction of the incoming current through N_1, which leads to a broadening of the skipping orbit trajectories. In Fig. 3a the center contact S is normal ($\Delta = 0$). A large portion of the injected current is then extracted through S. In contrast, when S is in the superconducting state, as shown in Fig. 3b, the current density increases substantially between S and N_2 due to CAR.

The technology to manufacture good contacts between superconducting metals and 2DEGs has been developed for several types of heterostructures [31, 32]. Although experimentally challenging due to the presence of important Schottky barriers, fairly high transparencies have been reported (for instance transmission probability $\sim$ 0.55 with a critical field of 2T in the In-GaAs heterostructures interfaces presented in Ref. 32). In Fig. 4, we show

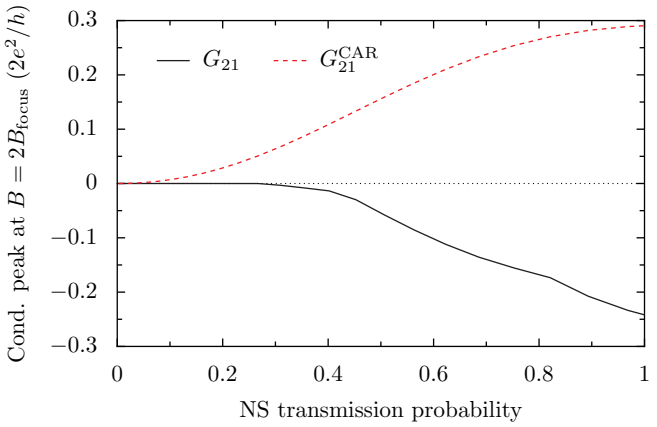

FIG. 4. (Color online) Magnitude of peak in G_{21} and $G_{21}^{\rm CAR}$ at $B/B_{\rm focus} = 2$ as a function of transmission probability of the interface between the 2DEG and the superconductor. The conductance is calculated at zero temperature.

the height of the CAR peak at $B/B_{\rm focus} = 2$ (for $T = 0$) as a function of the transmission probability of the NS contact. The CAR peak diminishes with decreasing quality of the interface but not dramatically so. We conclude that the effect should be observable with the available technology.

In conclusion, we have shown that electron focusing can be used to enhance CAR over length scales much larger than the superconducting coherence length ξ. The limiting length scale for electron focusing and therefore CAR enhancement, is the mean free path $l_{\rm mf}$, which can be several orders of magnitude larger than ξ [12, 15]. CAR is enhanced at the cost of ET for magnetic fields that are integer multiples of the focusing field in Eq. (2). At half integer multiples of the focusing field, CAR plays a negligible role since the electron orbits avoid the superconducting contact. Instead ET is enhanced as in normal electron focusing [15]. The necessary magnetic field is relatively weak, and should be an easily accessible experimental "knob" for controlling the CAR enhancement.

CAR has been proposed as a means to create a solid state entangler, using the natural entanglement of Cooper pairs. However, in most systems quasiparticle backscattering into the injector contacts is a serious limitation [33]. This difficulty does not exist in our scheme.

This work was supported by The Research Council of Norway through grant no. 167498/V30.

[1] J. M. Byers and M. E. Flatté, Phys. Rev. Lett, **74**, 306 (1995).
[2] G. Deutscher and D. Feinberg, Appl. Phys. Lett., **76**, 487 (2000).
[3] G. Falci, D. Feinberg, and F. W. J. Hekking, Europhys. Lett., **54**, 255 (2001).
[4] D. Feinberg, Eur. Phys. J. B, **36**, 419 (2003).
[5] P. Recher, E. V. Sukhorukov, and D. Loss, Phys. Rev. B, **63**, 165314 (2001).
[6] S. G. den Hartog, C. M. A. Kapteyn, B. J. van Wees, T. M. Klapwijk, and G. Borghs, Phys. Rev. Lett, **77**, 4954 (1996).
[7] D. Beckmann, H. B. Weber, and H. v. Löhneysen, Phys. Rev. Lett, **93**, 197003 (2004).
[8] S. Russo, M. Kroug, T. M. Klapwijk, and A. F. Morpurgo, Phys. Rev. Lett, **95**, 027002 (2005).
[9] J. P. Morten, A. Brataas, and W. Belzig, Phys. Rev. B, **74**, 214510 (2006); J. P. Morten, D. Huertas-Hernando, W. Belzig, and A. Brataas, *ibid.*, **78,**, 224515 (2008).
[10] P. Cadden-Zimansky and V. Chandrasekhar, Phys. Rev. Lett, **97**, 237003 (2006).
[11] P. Cadden-Zimansky, J. Wei, and V. Chandrasekhar, Nat. Phys., **5**, 393 (2009).
[12] A. Levy Yeyati, F. S. Bergeret, A. Martín-Rodero, and T. M. Klapwijk, Nat. Phys., **3**, 455 (2007).
[13] D. S. Golubev, M. S. Kalenkov, and A. D. Zaikin, Phys. Rev. Lett, **103**, 067006 (2009).
[14] J. Wei and V. Chandrasekhar, Nat. Phys., **6**, 494 (2010).
[15] H. van Houten, C. W. J. Beenakker, J. G. Williamson, M. E. I. Broekaart, P. H. M. van Loosdrecht, B. J. van Wees, J. E. Mooij, C. T. Foxon, and J. J. Harris, Phys. Rev. B, **39**, 8556 (1989).
[16] C. W. J. Beenakker, H. van Houten, and B. J. van Wees, Superlattices Microstruct., **5**, 127 (1989).
[17] K. Bolotin, K. Sikes, Z. Jiang, M. Klima, G. Fudenberg, J. Hone, P. Kim, and H. Stormer, Solid State Commun., **146**, 351 (2008).
[18] F. Chen, J. Xia, and N. Tao, Nano Lett., **9**, 1621 (2009).
[19] P. A. M. Benistant, H. van Kempen, and P. Wyder, Phys. Rev. Lett, **51**, 817 (1983).
[20] V. S. Tsoi, J. Bass, and P. Wyder, Rev. Mod. Phys., **71**, 1641 (1999).
[21] F. Giazotto, M. Governale, U. Zülicke, and F. Beltram, Phys. Rev. B, **72**, 054518 (2005).
[22] S. I. Bozhko, V. S. Tsoi, and S. E. Yakovlev, Pis'ma Zh. Eksp. Teor. Fiz, **36**, 123 (1982), [JETP Lett. 36, 152 (1982)].
[23] P. K. Polink, C. J. Lambert, J. Koltai, and J. Cserti, Phys. Rev. B, **74**, 132508 (2006).
[24] P. Rakyta, A. Kormanyos, Z. Kaufmann, and J. Cserti, Phys. Rev. B, **76**, 064516 (2007).
[25] H. J. Niu and D. P. Hampshire, Phys. Rev. Lett, **91**, 027002 (2003).
[26] Y. Nambu, Phys. Rev., **117**, 648 (1960).
[27] H. Hoppe, U. Zülicke, and G. Schön, Phys. Rev. Lett, **84**, 1804 (2000).
[28] K. Kazymyrenko and X. Waintal, Phys. Rev. B, **77**, 115119 (2008).
[29] D. P. Lide, ed., *CRC Handbook of Chemistry and Physics*, 90th ed. (CRC Press, 2010).
[30] J. Bardeen, L. N. Cooper, and J. R. Schrieffer, Phys. Rev., **108**, 1175 (1957).
[31] H. Takayanagi and T. Kawakami, Phys. Rev. Lett, **54**, 2449 (1985).
[32] S. Boulay, J. Dufouleur, P. Roche, U. Gennser, A. Cavanna, and D. Mailly, J. Appl. Phys., **105**, 123919 (2009).
[33] J. P. Morten, D. Huertas-Hernando, W. Belzig, and A. Brataas, Europhys. Lett., **81**, 40002 (2008).